European Journal of Lipid Science and Technology

WILEY-VCH

European Journal of
Lipid Science and Technology

RESEARCH ARTICLE OPEN ACCESS

Catalytic Dehydrogenation of Lauric Acid and a Potential Use in Polyester Synthesis

Luis Santos Correa[1] | Emma Stapf[2] | Timo Nonner[2] | Michael A. R. Meier[1,2]

[1]Laboratory of Applied Chemistry, Institute of Biological and Chemical Systems – Functional Molecular Systems (IBCS-FMS), Karlsruhe Institute of Technology (KIT), Eggenstein-Leopoldshafen, Germany | [2]Laboratory of Applied Chemistry, Institute of Organic Chemistry (IOC), Karlsruhe Institute of Technology (KIT), Karlsruhe, Germany

Correspondence: Michael A. R. Meier (m.a.r.meier@kit.edu)

Received: 4 December 2024 | **Revised:** 10 January 2025 | **Accepted:** 4 February 2025

Funding: The authors received no specific funding for this work.

Keywords: dehydrogenation | green chemistry | polyesters | saturated fatty acids | thia-Michael addition

ABSTRACT

The substitution of depleting fossil resources by renewable resources is of paramount importance, especially for polymer chemistry with its large production volume, in order to guarantee a more sustainable future. Herein, a new three-step reaction sequence was developed to synthesize renewable fatty acid–based dimethyl esters from saturated fatty acids. The sequence consists of a catalytic dehydrogenation with molecular oxygen as oxidant, an esterification with methanol, and a dimerization reaction with dithiols via thia-Michael addition. Three new dimethyl esters were thus synthesized from lauric acid and fully characterized via infrared, ^{1}H NMR, and ^{13}C NMR spectroscopy as well as mass spectrometry. Polyesters with molecular weights ranging from 26.0 to 31.8 kDa were obtained by polycondensation of each dimethyl ester with 1,12-dodecanediol. Methyl crotonate–based polymers were prepared for comparison with the fatty acid–derived materials. Thermogravimetric analysis revealed that the long side chains led to improved thermal stability, and differential scanning calorimetry showed side chain crystallization for one polymer.

Practical Applications Renewable dimethyl esters are valuable monomers for the sustainable synthesis of polyesters and polyamides. The herein-reported synthesis strategy valorized saturated fatty acids, a typically less useful resource for polymer chemistry.

1 | Introduction

The substitution of depleting fossil resources by renewable and more sustainable materials is crucial. Especially research on polymers must implement renewable resources, as to date still less than 1% of the worldwide production of plastics is bio-based [1]. Fatty acids and plant oils are the most valuable feedstock for the production of bio-based polymers. Unsaturated fatty acids, such as oleic acid, linoleic acid, and linolenic acid, are easily functionalized at their double bonds by oxidations, thiol-ene reactions, olefin metathesis, or isomerizing functionalization to synthesize difunctional monomers for the synthesis of various polymers [2, 3]. Functionalization of plant oil triglyceride double bonds yields polyfunctional derivatives that are used for the synthesis of cross-linked materials [4]. In contrast, the chemistry of saturated fatty acids is mainly restricted to the carboxylic acid moiety and therefore less versatile. Esterification of saturated fatty acids is a common approach to either introduce new

Abbreviations: DMSO, dimethyl sulfoxide; ESI, electrospray ionization; IR, infrared spectroscopy; MS, mass spectrometry; NMR, nuclear magnetic resonance; PTFE, poly(tetrafluoroethylene); ^{t}Amyl-OH, *tert*-amyl alcohol; ^{t}BuOH, *tert*-butanol; TLC, thin-layer chromatography; DBN, 1,5-diazabicyclo[4.3.0]non-5-ene; DBU, 1,8-diazabicyclo[5.4.0]undece-7-ene; TBD, 1,5,7-triazabicyclo[4.4.0]dec-5-ene; TMG, 1,1,3,3-tetramethylguanidine.

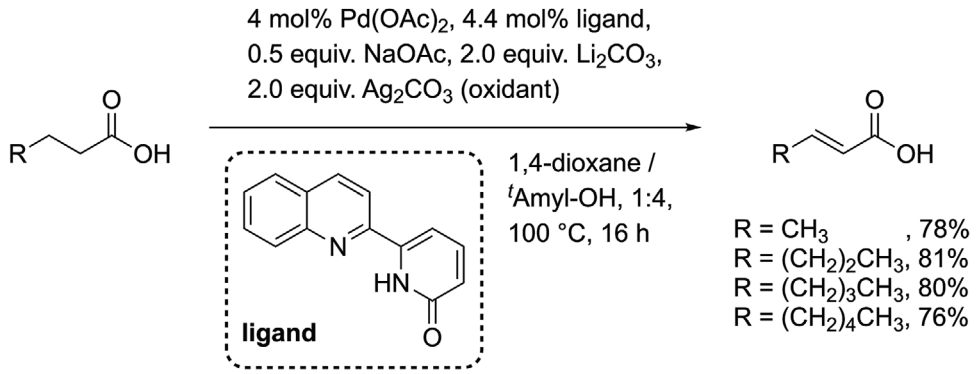

SCHEME 1 | Ligand-controlled palladium-catalyzed dehydrogenation of aliphatic carboxylic acids [12].

functional groups (e.g., double bonds) or increase the acidity of α-CH_2 protons (e.g., methyl ester) and hence enable further functionalization through enolate chemistry. Radical polymerization and ring-opening metathesis polymerization can be performed with fatty acid vinyl esters [5–7] and fatty acid norbornene esters [8], respectively. One example for the use of enolate chemistry is the synthesis of fatty acid–derived dimethyl malonates from fatty acid methyl ester enolates and dimethyl carbonate [9]. The synthesized dimethyl malonates were subsequently polymerized with 1,6-hexanediol to synthesize polyesters with aliphatic side chain lengths between 6 and 16 carbon atoms and molecular weights between 9 and 17 kDa. Another pathway to saturated fatty acid–derived dimethyl esters suitable for polymerizations is the oxidative coupling of fatty acid enolates with copper(II) bromide as oxidant [10].

The introduction of double bonds into the carbon chain of saturated fatty acids is desirable to allow for further modification and thus increase the scope of their applications. However, not many methods have been developed so far due to the difficulty of selectively activating methylene $C(sp^3)$–H bonds in the molecule, while simultaneously preventing $C(sp^2)$–H activation of the products' more reactive double bond. One example for a selective dehydrogenation of aliphatic carboxylic acids was reported by Newhouse et al. [11]. In this method, α,β-unsaturated carboxylic acids were obtained in high yields (>80%) through the dehydrogenation of zinc enediolates by palladium(II) complexes with allyl acetate as the final oxidant [11]. The procedure itself is, however, impractical on large scale and rather unsustainable, as highly reactive *n*-butyllithium and a protective gas atmosphere are required for the synthesis of the used zinc enediolates. Recently, Yu et al. reported another palladium-catalyzed dehydrogenation method for the synthesis of α,β-unsaturated carboxylic acids from saturated precursors (Scheme 1) [12]. The development of this dehydrogenation procedure was possible through the careful design of pyridine–pyridone ligands with different bite angles. Hence, five-membered chelating ligands selectively formed the desired α,β-unsaturated product, whereas six-membered chelating ligands further reacted in $C(sp^2)$–H activation of the products' double bond in a tandem reaction [12]. In contrast to the procedure from Newhouse, neither protective gas atmosphere nor highly reactive substances were needed. Moreover, it was demonstrated that molecular oxygen can be used as a final oxidant to further increase the sustainability of the procedure. The dehydrogenation achieved yields higher than 75% for linear aliphatic carboxylic acids with chain lengths up to octanoic acid if silver carbonate was used as an oxidant [12]. Longer chain fatty acids were not investigated for this reaction.

We, therefore, reasoned that this dehydrogenation procedure might be useful for the synthesis of long-chain α,β-unsaturated fatty acids (C_{12} to C_{18}). Dimerization of these compounds gives access to dimethyl esters and therefore to the synthesis of bio-based polyesters. We considered the thia-Michael addition to be the most suitable reaction for this dimerization, as it can be performed in a sustainable manner to achieve near-quantitative yields with low catalyst loadings at room temperature [13–15]. The thia-Michael addition is tolerant toward functional groups and can be catalyzed by various compounds, such as Lewis acids [16, 17], Brønsted acids [18, 19], nucleophiles [20, 21], and Brønsted bases [22–24].

Thus, we herein report the synthesis of renewable dimethyl esters from lauric acid by the combination of the palladium-catalyzed dehydrogenation procedure from Yu et al. with the thia-Michael addition of aliphatic dithiols. First, the dehydrogenation was optimized to produce α,β-unsaturated lauric acid in a more sustainable manner. The unsaturated carboxylic acid was then esterified with methanol to enable the subsequent thia-Michael addition of 1,4-butanedithiol, 1,6-hexanedithiol, and 1,10-decanedithiol for the synthesis of three dimethyl esters. Finally, polyesters were synthesized by polymerization of all dimethyl esters with renewable 1,12-dodecanediol [25].

2 | Materials and Methods

2.1 | Materials

All starting materials, solvents, and reagents were purchased from chemical suppliers and used without further purification unless stated otherwise.

2.1.1 | Used Solvents

Cyclohexane (VWR, HPLC grade), 1,4-dioxane (Sigma-Aldrich, 99.8%), ethanol (Thermo Fisher Scientific, HPLC grade), ethyl acetate (VWR, HPLC grade), methanol (Thermo Fisher Scientific, HPLC grade), *tert*-amyl alcohol (^{t}Amyl-OH) (Sigma-Aldrich,

99%), and *tert*-butanol (^{t}BuOH) (Acros Organics, 99.5%) were used without further purification. Dichloromethane (OQEMA, technical) was purified by distillation prior to use. Deuterated solvents, that is, dimethyl sulfoxide (DMSO)-d_6 (<99.8% D) and $CDCl_3$ (<99.8% D), were purchased from Eurisotop.

2.1.2 | Used Compounds

2-Acetyl-6-bromopyridine (ChemPUR, 98%), anthranilaldehyde (abcr, 95%), 1,4-butanedithiol (Sigma-Aldrich, 98%), cerium(IV) sulfate (ChemPUR, 98%), cesium carbonate (Sigma-Aldrich, 99%), 18-crown-6 (abcr, 99%), 1,10-decanedithiol (Tokyo Chemical Industry, >98%), 1,8-diazabicyclo[5.4.0]undece-7-ene (DBU) (Fluorochem, 98%), 1,5-diazabicyclo[4.3.0]non-5-ene (DBN) (Thermo Scientific Chemicals, 98%), dibromomethane (Sigma-Aldrich, ≥98.5%), 1,12-dodecanediol (Thermo Scientific, 98%), formic acid (Acros Organics, 99%), 1,6-hexanedithiol (abcr, 97%), lauric acid (Thermo Scientific, 99%), lithium carbonate (Tokyo Chemical Industry, >98%), magnesium sulfate (Carl Roth, ≥99%), 4-methoxybenzylalcohol (Sigma-Aldrich, 98%), methyl crotonate (Sigma-Aldrich, 98%) myristic acid (Sigma-Aldrich, for synthesis), octanoic acid (Sigma-Aldrich, ≥99%), palladium(II) acetate (Sigma-Aldrich, for synthesis), palmitic acid (Sigma-Aldrich, for synthesis), phosphomolybdic acid (Sigma-Aldrich, >99%), potassium carbonate (Sigma-Aldrich, >99%), potassium hydroxide (Honeywell, ≥85%), potassium permanganate (Sigma-Aldrich, >99%), pyridine (Sigma-Aldrich, >99%), silver carbonate (ChemPUR, 99.7%), sodium acetate (Bernd Kraft, for analysis), sodium carbonate (Thermo Scientific, 99.5%), sodium chloride (Sigma-Aldrich, >99%), sodium hydroxide (Sigma-Aldrich, >99%), sodium sulfate (Thermo Fisher Scientific, 99%), stearic acid (abcr, 98%), sulfuric acid (Sigma-Aldrich, 98%), 1,1,3,3-tetramethylguanidine (TMG) (Thermo Scientific, 99%), titanium(IV) isopropoxide (Sigma-Aldrich, 97%), and triethylamine (Fluorochem, for synthesis) were used without further purification.

2.2 | Methods

2.2.1 | Thin-Layer Chromatography (TLC)

Aluminum plates coated with fluorescent silica gel of the type F_{254} obtained from Sigma-Aldrich were used for TLC measurements. TLC plates with the applied samples were placed in a glass chamber filled with eluent (filling height ca. 0.5 cm). The plates were removed once the eluent front had reached a height of ~3 cm and cautiously dried with a heat gun. The compounds on the plates were visualized by either potassium permanganate stain (solution of 1.5 g potassium permanganate, 10 g potassium carbonate, 1.25 mL sodium hydroxide solution [10 wt%], and 200 mL water) or Seebach stain (2.0 g cerium(IV) sulfate, 5.0 g phosphomolybdic acid, 16 mL sulfuric acid, and 200 mL water).

2.2.2 | Flash Column Chromatography

The purification of compounds by flash column chromatography was conducted according to the publication of Still et al. [26]. Silica gel, obtained from Sigma Aldrich, with a pore size of 60 Å, a mesh size of 230–240, and a particle size of 40–63 μm, was used as the stationary phase.

2.2.3 | Distillation

A Büchi Labortechnik Kugelrohr model B-585 was used for distillations of volumes smaller than 5 mL.

2.3 | Instruments

2.3.1 | Infrared (IR) Spectroscopy

IR spectra of all compounds were recorded on a Bruker Alpha Fourier transform IR spectrometer with attenuated total reflection (ATR) technology in the range from 4000 to 400 cm^{-1}. The resulting absorbance spectra are averaged over 24 scans per measurement. By convention, the signals are noted from large to small wavenumbers. Characterization of the absorption bands was done in dependence of the absorption strength with the following abbreviations: vs (very strong), s (strong), m (medium), w (weak), and vw (very weak).

2.3.2 | Nuclear Magnetic Resonance (NMR) Spectroscopy

^{1}H NMR spectra were recorded either on a Bruker Ascend 400 spectrometer at 400 MHz with 16 scans and a delay time D_1 of 1 s at 298 K or on a Bruker Avance DRX spectrometer at 500 MHz with 16 scans and a delay time D_1 of 1 s at 298 K. The chemical shift δ is reported in parts per million and referenced to the solvent signal of DMSO-d_5 at 2.50 ppm or $CHCl_3$ at 7.26 ppm. Additionally, gradient-selected correlation spectroscopy (COSY) was carried out for signal assignment of protons. The following abbreviations are used to describe the proton splitting pattern: s = singlet, d = doublet, t = triplet, m = multiplet. All coupling constants J are given in Hz and decreasing order. ^{13}C NMR spectra were recorded either on a Bruker Ascend 400 spectrometer at 101 MHz with 1024 scans and a delay time D_1 of 2 s at 298 K or on a Bruker Avance DRX spectrometer at 126 MHz with 1024 scans and a delay time D_1 of 2 s at 298 K. The chemical shift δ is reported in parts per million and referenced to the solvent signal of DMSO-d_6 at 39.52 ppm or $CDCl_3$ at 77.16 ppm. Furthermore, phase-edited heteronuclear single-quantum coherence ($HSQC_{ed}$) and heteronuclear multiple-bond correlation (HMBC) spectroscopy were carried out for signal assignment of carbon atoms and structure elucidation. Signals of carbon atoms were specified as follows: C_q = quaternary carbon atom, CH, CH2, or CH3.

2.3.3 | Mass Spectrometry (MS)

Electrospray ionization (ESI) experiments were recorded on a Q Exactive Plus (Orbitrap) mass spectrometer (Thermo Fisher Scientific) equipped with a HESI II probe to record high resolution. The spectra of most compounds were evaluated by molecular signals $[M]^+$, signals of protonated molecules $[M + H]^+$, signals of adducts such as $[M + Na]^+$, and characteristic fragment peaks and indicated with their mass-to-charge ratio (m/z). Moreover, spectra

of carboxylic acids were evaluated by signals of deprotonated molecules $[M–H]^-$.

2.3.4 | Size Exclusion Chromatography (SEC)

SEC analyses were performed on a Shimadzu Size Exclusion Chromatography system equipped with a Shimadzu isocratic pump model LC-20AD, a Shimadzu autosampler model SIL-20A, and a Shimadzu refractive index detector model RID-20A. A mixture of anhydrous tetrahydrofuran stabilized with 250 ppm butylated hydroxytoluene (BHT, ≥99.9%) and triethylamine (2 vol% of THF) was used at a flow rate of 1.0 mL min^{-1} and at 30°C as a mobile phase. The analysis was performed on the following column system: PSS SDV analytical precolumn (5 µm, 8 mm × 50 mm), PSS SDV analytical column (5 µm, 8 mm × 300 mm, 1000 Å), and a PSS SDV analytical column (5 µm, 8 mm × 300 mm, 100 000 Å). For the calibration, narrow linear poly(methyl methacrylate) standards (Polymer Standards Service, PSS, Germany) ranging from 1100 to 981 000 Da were used. For sample preparation, 2.00 mg of analyte was dissolved in 1.50 mL of the solvent mixture used in the system. Unless stated otherwise, the samples were dissolved at room temperature for 30 min until a transparent solution was obtained and afterward filtered by syringe filter prior to use to avoid plugging of the injection setup or the column.

2.3.5 | Differential Scanning Calorimetry (DSC)

DSC measurements were recorded on a 214 Polyma DSC device from NETZSCH (Selb, Germany). All experiments were carried out under a nitrogen atmosphere using 40 µL aluminum crucibles and a sample mass of 4–7 mg. The samples were measured using the following program: first heating from −150 to 200°C, then cooling from 200 to −150°C, and a final heating step from −150 to 200°C with a heating/cooling rate of 10 K min^{-1}. The glass transition temperature (T_g) and the temperature of phase transitions like cold crystallization (T_{cc}) and melting point (T_m) were determined from the second heating run to eliminate possible interference from the polymer's thermal history.

2.3.6 | Thermogravimetric Analysis (TGA)

TGA measurements were performed on a TA Instruments TGA 5500 under a nitrogen atmosphere using platinum TGA sample pans and a heating rate of 10 K min^{-1} over a temperature range from 25 to 600°C. $T_{d,5\%}$ is defined as the temperature of 5% weight loss.

2.4 | Procedures

2.4.1 | Ligand Synthesis

The synthesis of the ligand 6-(quinolin-2-yl)pyridin-2(1*H*)-one was conducted according to the literature and is described in detail in the Supporting Information section 1.1 [12].

2.4.2 | Dehydrogenation of Fatty Acids With Silver Carbonate as Oxidant [12]

The carboxylic acid (i.e., octanoic, lauric, myristic, palmitic, or stearic acid) (700 µmol, 1.00 equiv.), silver carbonate (386 mg, 1.40 mmol, 2.00 equiv.), lithium carbonate (103 mg, 1.40 mmol, 2.00 equiv.), and sodium acetate (28.7 mg, 350 µmol, 0.50 equiv.) were weighed into a 10 mL screw-cap vial. A solution of palladium(II) acetate (6.29 mg, 28.0 µmol, 4.00 mol%) and 6-(quinolin-2-yl)pyridin-2(1*H*)-one (6.85 mg, 30.8 µmol, 4.40 mol%) in 1,4-dioxane (1.40 mL) was premixed and added to the tube. Then, ^{t}Amyl-OH (5.60 mL) was added, and the tube was briefly flushed with argon, and the vial was capped. The reaction mixture was then stirred at the rate of 300 rpm at 100°C for 16 h. After cooling to room temperature, the mixture was acidified with formic acid (158 µL, 4.20 mmol, 6.00 equiv.). The mixture was passed through a pad of Celite with a solvent mixture (methanol/formic acid/dichloromethane, 5:5:90) as the eluent to remove any insoluble precipitate. The solvent of the filtrate was removed under reduced pressure, and a ^{1}H NMR spectrum was measured in $CDCl_3$.

2.4.3 | Lauric Acid Dehydrogenation in ^{t}BuOH/H_2O With Oxygen as Oxidant

Lauric acid (100 mg, 500 µmol, 1.00 equiv.) and the respective base were dissolved in a mixture of ^{t}BuOH and water (10 mL, 1:1). Palladium(II) acetate (4.49 mg, 20.0 µmol, 4.00 mol%) and 6-(quinolin-2-yl)pyridin-2(1*H*)-one (4.89 mg, 22.0 µmol, 4.40 mol%) were added and the mixture was stirred at 60°C until all compounds dissolved. Then, the solution was added to a 50 mL poly(tetrafluoroethylene) (PTFE) inlet of a pressure reactor. The pressure reactor was sealed, and the reaction mixture was stirred at the rate of 600 rpm at the respective temperature under pure oxygen atmosphere (10 bar) for 24 h. After cooling to room temperature, the mixture was acidified with formic acid (57.2 µL, 1.50 mmol, 3.00 equiv.) and diluted with water (10 mL). The reaction mixture was extracted with dichloromethane (3 × 15 mL). The combined organic layers were washed with saturated sodium chloride solution (2 × 10 mL), dried over sodium sulfate, filtered, and the solvent was removed under reduced pressure. A ^{1}H NMR spectrum was measured in $CDCl_3$ after the addition of dibromomethane (9.00 µL, 22.3 mg, 128 µmol, 0.26 equiv.) as an external standard to determine the reaction yield (see Figure S10 for an exemplary ^{1}H NMR spectrum).

2.4.4 | Solvent-Free Dehydrogenation of Lauric Acid With Oxygen as Oxidant

Lauric acid (40.1 g, 200 mmol, 1.00 equiv.), palladium(II) acetate (1.80 g, 8.00 mmol, 4.00 mol%), and 6-(quinolin-2-yl)pyridin-2(1*H*)-one (1.96 g, 8.80 mmol, 4.40 mol%) were added into a 150 mL PTFE inlet of a pressure reactor. The pressure reactor was sealed, and the reaction mixture was stirred at the rate of 600 rpm at 100°C under pure oxygen atmosphere (10 bar) for 24 h. The reaction mixture was distilled in vacuo in a Kugelrohr oven (150°C, 0.1 mbar) to obtain a mixture of lauric acid and α,β-

unsaturated lauric acid in a ratio of 60:40, as determined by ^{1}H NMR spectroscopy (38.6 g, 195 mmol, 97%) (Figure S12).

2.4.5 | Esterification of Mixture of Lauric Acid and α,β-Unsaturated Lauric Acid With Methanol

The mixture of lauric acid and α,β-unsaturated lauric acid (38.5 g, 194 mmol, 1.00 equiv.), methanol (315 mL, 7.77 mol, 40.0 equiv.), and sulfuric acid (96%, 1.08 mL, 19.4 mmol, 10 mol%) was added into a 500 mL round bottom flask. The reaction solution was stirred at 65°C for 4 h. After cooling to room temperature, the solvent methanol was removed under reduced pressure. The residue was diluted with ethyl acetate (200 mL) and washed with water (2 × 100 mL) and saturated sodium chloride solution (100 mL). The organic phase was dried over sodium sulfate, filtered, and the solvent was removed under reduced pressure to obtain a mixture of methyl laurate and α,β-unsaturated methyl laurate in a ratio of 60:40, as determined by ^{1}H NMR spectroscopy (39.1 g, 184 mmol, 95%) (Figure S14).

2.4.6 | Thia-Michael Addition of 1,4-Butanedithiol to α,β-Unsaturated Methyl Laurate

α,β-Unsaturated methyl laurate (40% NMR purity, 39.0 g, 73.5 mmol, 1.00 equiv.), 1,4-butanedithiol (97%, 4.63 g, 4.44 mL, 36.7 mmol, 0.50 equiv.), and TMG (277 µL, 254 mg, 2.20 mmol, 3.00 mol%) were mixed at room temperature, and the mixture was then stirred for 16 h at 80°C. After cooling to room temperature, the reaction mixture was diluted with ethyl acetate (200 mL) and acidified with 2 M hydrochloric acid. The organic phase was washed with water (2 × 100 mL) and saturated sodium chloride solution (100 mL), dried over sodium sulfate, filtered, and the solvent was removed under reduced pressure. The crude product was distilled in vacuo (100°C, 0.1 mbar) to recover the unreacted methyl laurate (21.7 g, 101 mmol, 93%). The residue of the distillation was purified by flash column chromatography (cyclohexane/ethyl acetate, 40:1) to obtain the title compound (15.0 g, 27.4 mmol, 75%). Analytical data for methyl laurate dimer **LD1**: ^{1}H NMR (500 MHz, $CDCl_3$, ppm): $\delta = 3.68$ (s, 6H), 3.01 (qd, $J = 7.3$, 5.7 Hz, 2H), 2.55 (d, $J = 7.2$ Hz, 4H), 2.54–2.48 (m, 4H), 1.69–1.63 (m, 4H), 1.59–1.49 (m, 4H), 1.48–1.33 (m, 4H), 1.32–1.19 (m, 24H), 0.87 (t, $J = 7.0$ Hz, 6H); ^{13}C NMR (126 MHz, $CDCl_3$, ppm): $\delta = 172.3$ (C_q, C_{Ester}), 51.8 (CH_3, C_{Ester}), 42.0 (CH, β-C_{Ester}), 41.0 (CH_2, α-C_{Ester}), 35.3 (CH_2), 32.0 (CH_2), 30.3 (CH_2), 29.7 (CH_2), 29.6 (CH_2), 29.6 (CH_2), 29.4 (CH_2), 29.0 (CH_2), 26.9 (CH_2), 22.8 (CH_2), 14.2 (CH_3); IR (ATR, cm^{-1}): $\tilde{\nu} = 2949$ (w), 2922 (vs), 2853 (m), 1737 (vs), 1458 (w), 1435 (m), 1354 (w), 1307 (w), 1279 (w), 1237 (m), 1221 (m), 1153 (s), 1125 (w), 1017 (w), 986 (vw), 881 (vw), 841 (vw), 722 (w); ESI-MS ($[M + H]^+$, $C_{30}H_{59}O_4S_2$) calcd.: 547.3849; found: 547.3848.

2.4.7 | General Procedure for Optimization of the Thia-Michael Addition

A mixture of methyl crotonate (98%, 511 mg, 5.00 mmol, 1.00 equiv.) 1,4-butanedithiol (97%, 309 mg, 2.50 mmol, 0.50 equiv.), and the respective catalyst (Table 3) was stirred in a 10 mL screw-cap vial at either room temperature or 90°C. ^{1}H NMR spectra of the reaction mixture were measured after certain time intervals in $CDCl_3$ to monitor the conversion of methyl crotonate (Table 3, Figures S19 and S20).

2.4.8 | General Procedure for Thia-Michael Additions of Dithiols to Methyl Crotonate

Methyl crotonate (1.00 equiv.), the respective dithiol (0.50 equiv.), and TMG (1.00 mol%) were mixed and stirred for 4 h at room temperature. The reaction mixture was diluted with ethyl acetate (50 mL) and acidified with 2 M hydrochloric acid. The organic phase was washed with water (2 × 50 mL) and saturated sodium chloride solution (50 mL), dried over magnesium sulfate, filtered, and the solvent was removed under reduced pressure. The crude product was purified either by distillation or by flash column chromatography (cyclohexane/ethyl acetate). Exemplary analytical data for methyl crotonate dimer **CD1** (data of **CD2** and **CD3** can be found in the Supporting Information section): ^{1}H NMR (400 MHz, $CDCl_3$, ppm): $\delta = 3.67$ (s, 6H), 3.17 (dp, $J = 8.3$, 6.7 Hz, 2H), 2.60 (dd, $J = 15.4$, 6.3 Hz, 2H), 2.57–2.50 (m, 4H), 2.43 (dd, $J = 15.4$, 8.1 Hz, 2H), 1.72–1.62 (m, 4H), 1.30 (d, $J = 6.8$ Hz, 6H); ^{13}C NMR (101 MHz, $CDCl_3$, ppm): $\delta = 172.0$ (C_q, C_{Ester}), 51.8 (CH_3, C_{Ester}), 42.2 (CH_2, α-C_{Ester}), 36.3 (CH, β-C_{Ester}), 30.3 (CH_2), 28.8 (CH_2), 21.6 (CH_3); IR (ATR, cm^{-1}): $\tilde{\nu} = 2951$ (w), 2927 (vw), 2866 (vw), 1732 (vs), 1435 (w), 1375 (vw), 1356 (w), 1299 (w), 1283 (w), 1221 (m), 1187 (w), 1157 (vs), 1109 (w), 1077 (w), 1023 (w), 996 (w), 880 (vw), 839 (vw), 742 (vw), 657 (vw), 594 (vw); ESI-MS ($[M + H]^+$, $C_{14}H_{27}O_4S_2$) calcd.: 323.1345; found: 323.1343.

2.4.9 | Alternative Synthesis of α,β-Unsaturated Lauric Acid

α,β-Unsaturated lauric acid was synthesized from decanal and malonic acid via a Knoevenagel–Doebner condensation [27]. Esterification with methanol and subsequent thia-Michael additions yielded **LD1–LD3** (Section 1.7).

2.4.10 | General Procedure for Polymerizations of Dimethyl Esters With 1,12-Dodecanediol

Dimethyl ester (**CD1–CD3**, or **LD1–LD3**) (1.00 equiv.), 1,12-dodecanediol (1.00 equiv.), and titanium(IV) isopropoxide (5.00 mol%) were weighed into a 10 mL screw-cap vial. Methanol (2 mL) and dichloromethane (2 mL) were added, and the compounds were mixed for 10 min to obtain a homogeneous solution. The mixture was then transferred into a Schlenk tube equipped with a mechanical stirrer. The pressure was reduced to 700 mbar, and the reaction was stirred at 140°C for 3 h and then at 180°C for 15 h. Afterwards, the pressure was reduced to 100 mbar, and the reaction was stirred at 200°C for 1 h. The pressure was further reduced to 10 mbar, and the reaction was stirred for another 4 h at 200°C. After cooling to room temperature, the residue was dissolved in chloroform and precipitated in a cold methanol/chloroform mixture (2:1). The polymer was isolated by filtration and dried at 70°C and 10 mbar.

TABLE 1 | Carboxylic acid dehydrogenation performed with silver carbonate as oxidant.

Carboxylic acid	Starting material–to-product ratio	NMR-yield (%)
Octanoic acid (C_8)	18:82	82
Lauric acid (C_{12})	52:48	48
Myristic acid (C_{14})	70:30	30
Palmitic acid (C_{16})	86:14	14
Stearic acid (C_{18})	94:6	6

Note: Reaction yields were estimated via integration of characteristic proton signals in the ^{1}H NMR spectrum (Figures S5–S9).
Abbreviation: NMR, nuclear magnetic resonance.

3 | Results and Discussion

At first, the original palladium-catalyzed dehydrogenation procedure from Yu et al. was employed to octanoic acid and to four fatty acids (C_{12} to C_{18}) to assess whether the length of the aliphatic chain has an impact on the dehydrogenation efficiency of the catalyst (Scheme 1) [12]. The procedure uses 1,4-dioxane and ^{t}Amyl-OH as solvents, 2.50 equiv. of lithium carbonate and sodium acetate as bases to deprotonate the carboxylic acid, and 2.00 equiv. of silver carbonate as oxidant. For all five reactions, a high selectivity was observed in ^{1}H NMR spectroscopy as all proton signals were either assigned to the product or to the unreacted starting material (Figures S5–S9). The ratio of starting material to product was determined via ^{1}H NMR spectroscopy by integration of the α-CH_2 protons of the saturated acid at 2.35 ppm and the CH_2 protons adjacent to the double bond of the α,β-unsaturated acid at 2.22 ppm (Table 1). Moreover, the absence of side products allowed the reaction yield to be calculated directly from the ratio of starting material to product. The dehydrogenation of octanoic acid achieved an NMR yield of 82% and served as a control experiment to demonstrate reproducibility, as the same reaction was already performed in the original publication with a yield of 76% [12]. For the fatty acids, a lower reactivity was observed with an increasing chain length. Already for lauric acid (C_{12}), the NMR yield reduced drastically to 48% and further decreased steadily with increasing carbon chain length.

An optimization of the original reaction protocol was therefore desired to improve reaction yields. Moreover, it should be noted that the original dehydrogenation protocol is considered rather unsustainable due to the large amount of waste that is generated by 2.50 equiv. of inorganic bases and 2.00 equiv. of silver carbonate as oxidant. In fact, Yu et al. demonstrated that molecular oxygen can be used as an oxidant to substitute silver carbonate [12]. However, not only was the toxic solvent DMF used [28], but in addition stoichiometric amounts of toxic *p*-benzoquinone as a co-catalyst [29]. The herein conducted optimization therefore included the use of molecular oxygen as oxidant in combination with the more sustainable solvents ^{t}BuOH and water [30, 31]. Co-catalysts were fully excluded to reduce the amount of waste formed, and the equivalents of inorganic base were reduced to a minimum (Table 2). Reaction time and temperature of 24 h and 100°C, respectively, were initially kept identical to the original procedure. The first experiment showed that 1.00 equiv. of lithium carbonate was sufficient for the reaction to proceed (Entry 1). Moreover, no loss in reaction yield was observed when lithium carbonate was replaced by the more abundant sodium carbonate (Entry 2). Higher amounts of sodium carbonate led to phase separation due to an increased polarity of the aqueous phase and therefore resulted in heterogeneous reactions with reduced yields (Entries 2–5). Replacing sodium carbonate with potassium carbonate and cesium carbonate further increased the yield to 24.6% and 32.4%, respectively (Entries 6–7). As expected, a reduced reaction temperature resulted in a lower reaction yield of 16.1% (Entry 8).

A too-high temperature, however, led to lower yields due to the formation of side products (Entries 9–10, Figures S10 and S11). A prolonged reaction time of 72 h did not result in a significantly higher yield (37.9%, Entry 11). An increased reaction yield was observed with higher catalyst loadings (Entries 12–13). Hence, double and four times the amount of catalyst achieved yields of 58.8% and 80.3%, respectively. The very low concentration of 50 $mmol^{-1}$ seemed unsustainable and impractical, as 10 g of starting material would already require one liter of reaction volume, therefore generating large amounts of solvent waste. Several attempts to increase the concentration resulted in lower reaction yields, again presumably due to phase separation caused by the increased concentration of inorganic base.

It was therefore decided to exclude the inorganic base and the solvents to prevent phase separations. Indeed, neither solvents nor bases were actually needed for the reaction to proceed. Reacting molten lauric acid at 100°C with 4.0 mol% of palladium(II) acetate and 4.4 mol% of ligand under 10 bar of oxygen atmosphere resulted in a yield of 38.3%, which is comparable to the yield of 48% that was obtained with the silver carbonate procedure (Table 2, Entry 14 vs. Table 1, Entry 2). A higher catalyst loading, however, did not result in a higher yield for this solvent-free approach (Entry 15). For octanoic acid, a higher yield of 46% was achieved, again confirming the reduced reactivity of longer chain carboxylic acids (Entry 16).

In summary, with the solvent-free approach, toxic DMF, toxic benzoquinone, and overstoichiometric amounts of lithium carbonate were avoided, and thus, the amount of waste formed is reduced significantly. The reaction was performed again with 40 g of lauric acid to demonstrate its easy scalability. The black residue of the reaction was distilled in vacuo at 150°C and 0.1 mbar to separate the fatty acids from the catalyst. A light-yellow mixture consisting of lauric acid and α,β-unsaturated lauric acid in a ratio of 60:40 was obtained, as determined by ^{1}H NMR spectroscopy (Figure S12). Separation of both compounds was not possible due to their chemical and physical similarity. However, it was rationalized that separation and purification should be straightforward after conducting a double-bond-specific reaction to transform the α,β-unsaturated lauric acid into a new compound with different properties.

Thus, the thia-Michael addition was utilized as a specific reaction for α,β-unsaturated compounds [14, 15]. It is used for functional groups such as acrylates [32, 33], maleates, α,β-unsaturated

TABLE 2 | Optimization of the palladium catalyzed dehydrogenation of lauric acid with molecular oxygen.

Entry	Base		Temperature (°C)	NMR-yield with CH_2Br_2 as external standard (%)
	Base	Equiv.		
1	Li_2CO_3	1.00	100	17.6
2	Na_2CO_3	1.00	100	18.0
3	Na_2CO_3	1.25	100	19.3
4	Na_2CO_3	1.50	100	7.2
5	Na_2CO_3	2.00	100	6.2
6	K_2CO_3	1.00	100	24.6
7	Cs_2CO_3	1.00	100	32.4
8	Cs_2CO_3	1.00	90	16.1
9	Cs_2CO_3	1.00	115	19.5
10	Cs_2CO_3	1.00	130	0.9
11[a]	Cs_2CO_3	1.00	100	37.9
12[b]	Cs_2CO_3	1.00	100	58.8
13[c]	Cs_2CO_3	1.00	100	80.3
14[d]	—	—	100	38.3
15[d,b]	—	—	100	26.5
16[d,e]	—	—	100	46.0

Note: Reaction conditions were the following unless stated otherwise: 10 bar O_2, 4.0 mol% $Pd(OAc)_2$, 4.4 mol% ligand, 24 h of reaction time, concentration of 50 mmol L^{-1} in a mixture of *tert*-butanol and water (1:1).

Abbreviation: NMR, nuclear magnetic resonance.

[a]Reaction time of 72 h.

[b]Double the amount of catalyst and ligand were used.

[c]Four times the amount of catalyst and ligand was used.

[d]Solvent-free.

[e]Octanoic acid was used instead of lauric acid.

cyclic ketones [16, 23], as well as acyclic α,β-unsaturated ketones [16, 17]. Basic catalysts, such as triethylamine, 1,5,7-triazabicyclo[4.4.0]dec-5-ene (TBD), and DBU, are commonly employed for thia-Michael additions. It was therefore reasonable to first conduct an esterification with methanol to convert the mixture of lauric acid and α,β-unsaturated lauric acid into their corresponding methyl esters. Otherwise, more than 100 mol% of base catalyst would be needed as the first equivalent is directly neutralized by the free carboxylic acid moieties. Additionally, strong acids would be needed during work-up to protonate the carboxylic acid groups and hence generate stoichiometric amounts of ammonium salt as waste. The mixture of carboxylic acid was hence esterified with methanol and catalytic amounts of sulfuric acid. The esterification proceeded quantitatively and was further characterized by NMR and IR spectroscopy. In comparison to the ^{1}H NMR spectrum of the starting materials, two additional methyl ester signals at 3.72 and 3.66 ppm with an integral ratio of 40:60 indicate the successful esterification of the mixture of α,β-unsaturated lauric acid and lauric acid (Figure S14). Moreover, in the IR spectrum, the C=O vibration signal of the carboxylic acid moiety at 1696 cm^{-1} shifted to 1741 cm^{-1}, which is characteristic for ester groups.

After successful dehydrogenation and esterification, the synthesis of three methyl laurate–based dimers (**LD1–LD3)** via thia-Michael addition from α,β-unsaturated methyl laurate and three dithiols was performed (Scheme 2, top). This approach was chosen as it enables the subsequent synthesis of bio-based polyesters (Scheme 2, bottom). The three dithiols, 1,4-butanedithiol, 1,6-hexanedithiol, and 1,10-decanedithiol, were used to investigate the influence of the dithiol length on the final properties of the resulting polyesters.

The reaction conditions of the thia-Michael addition were, however, first optimized for the addition of 1,4-butanedithiol to methyl crotonate before transferring them to the α,β-unsaturated methyl laurate (Scheme 2, top). Reasoning for this was the commercial availability of methyl crotonate in a high purity of 98%, which simplified monitoring of the reaction in contrast to the mixture of methyl esters that was obtained from the dehydrogenation. First, triethylamine (NEt_3) was tested as a catalyst because it was reported to be efficient for thia-Michael additions of thiols to cyclohexenone and methyl acrylate [23, 32]. The reaction was performed with 10 mol% of NEt_3 and was stirred for 24 h at room temperature. It was possible to measure the ratio of methyl crotonate to the crotonate-based dimer **CD1** via ^{1}H NMR spectroscopy by integration of the double bond proton signal at 5.83 ppm and the signal of the newly formed thioether moiety at 3.18 ppm (Figure S19). Hence, a conversion of 29% was achieved with NEt_3 as a catalyst at room temperature, which could further be increased to 53% when the reaction was performed at 90°C (Table 3, Entries 1–2). The organic superbase

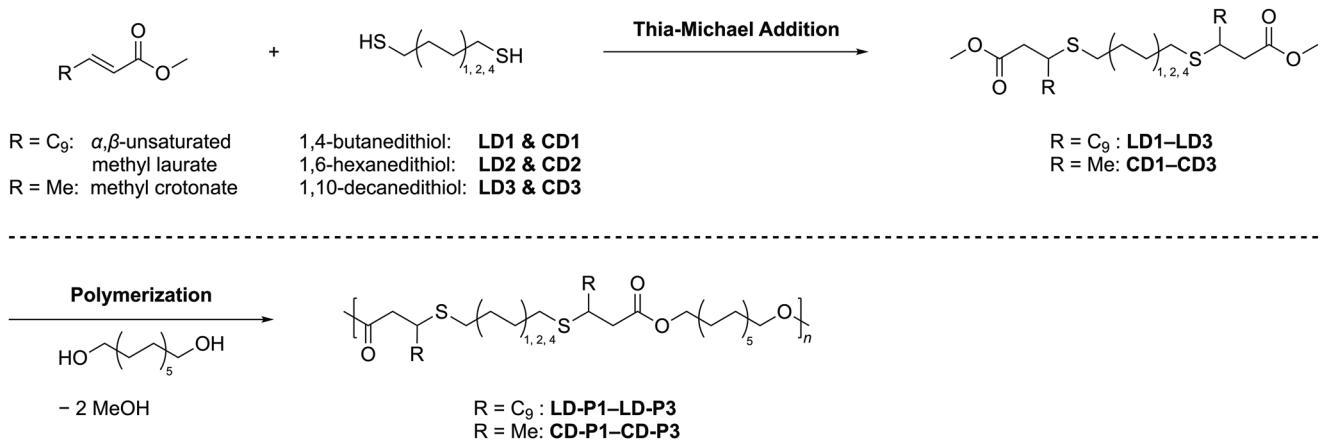

SCHEME 2 | Thia-Michael addition of dithiols to methyl crotonate and α,β-unsaturated methyl laurate to yield dimethyl esters (top) and polymerization with 1,12-dodecanediol (bottom).

TABLE 3 | Optimization of thia-Michael addition of 1,4-butanedithiol to methyl crotonate.

Entry	Catalyst	Time (h)	Methyl crotonate: product ratio determined by ^{1}H NMR spectroscopy
1	10 mol% NEt_3	24	71:29
2[a]	10 mol% NEt_3	24	47:53
3	10 mol% DBN	1	0:100
4	1 mol% DBN	1	26:74
		20	14:86
5	1 mol% DBU	2	02:98
6	1 mol% TMG	2	03:97

Abbreviations: DBN, 1,5-diazabicyclo[4.3.0]non-5-ene; DBU, 1,8-diazabicyclo[5.4.0]undece-7-ene; NMR, nuclear magnetic resonance, TMG, 1,1,3,3-tetramethylguanidine.
[a]Reaction was performed at 90°C.

DBN was tested as the next catalyst, as multiple reports in the literature described that such nitrogen bases were more active catalysts for thia-Michael additions than triethylamine [20, 21, 24]. Indeed, a conversion of 100% was achieved already after 1 h at room temperature with 10 mol% of DBN (Entry 3). It was therefore aimed to further decrease the catalyst loading to reduce the amount of waste formed. However, 1 mol% of DBN achieved a lower conversion of 86% after 20 h of reaction time (Entry 4). DBU was a more active catalyst at 1% loading and achieved a conversion of 98% after 2 h (Entry 5). DBU was, however, undesired as a catalyst for this reaction due to its expensiveness and, more importantly, its toxicity [34]. The cheaper and less toxic superbase TMG proved to be as effective as DBU with a conversion of 97% at 1% loading and was therefore chosen as a catalyst for all further reactions (Entry 6, Figure S20) [35, 36]. Purification of **CD1** was performed in a sustainable manner by distillation in vacuo to achieve a high yield of 93%. In ^{1}H NMR spectroscopy, characteristic signals of methyl ester and thioether moieties were observed at 3.68 and 3.17 ppm, respectively (Figure 1, top). Two diastereomeric protons were detected at 2.61 and 2.44 ppm due to the newly formed stereocenter, and protons of the 1,4-butanedithiol scaffold were detected at 2.54 and 1.67 ppm.

The structure of **CD1** was further confirmed by ^{13}C NMR spectroscopy, as characteristic signals of the quaternary ester carbon and the new thioether moiety were observed at 172 and 36.3 ppm, respectively (Figure S22). The two other methyl crotonate dimers, **CD2** and **CD3**, were obtained with the same procedure and obtained in yields of 94% and 84%, respectively. **CD2** was purified by distillation in vacuo, whereas **CD3** had to be purified by flash column chromatography due to its very high boiling point.

With TMG as the optimal catalyst, the thia-Michael addition of 1,4-butanedithiol was employed to the mixture of α,β-unsaturated methyl laurate and methyl laurate. The reaction was conducted with 3 mol% of TMG to ensure full conversion and stirred for 16 h at 80°C due to the reduced reactivity of the α,β-unsaturated methyl laurate compared to methyl crotonate. Noteworthy, it was possible to recover the unreacted methyl laurate by distillation in a yield of 93%, which corresponds to 51% of the initially used amount of lauric acid in the dehydrogenation step, thus minimizing waste generation. The initial separation issue of α,β-unsaturated lauric acid and lauric acid was therefore no longer present after the double-bond-specific thia-Michael reaction had been performed, as reasoned before. Methyl laurate dimer **LD1** was isolated from the distillation residue by flash column chromatography in a yield of 75%, which corresponds to an overall yield of 27% over the three reactions. In ^{1}H NMR spectroscopy, all characteristic signals that were observed for **CD1** were detected as well for **LD1** (Figure 1, bottom). The diastereomeric protons, however, appeared as one doublet in contrast to the two separated signals that were observed for **CD1**. The successful isolation of **LD1** was further confirmed by ^{13}C NMR and IR spectroscopy and MS (Supporting Information Section 1.3.3).

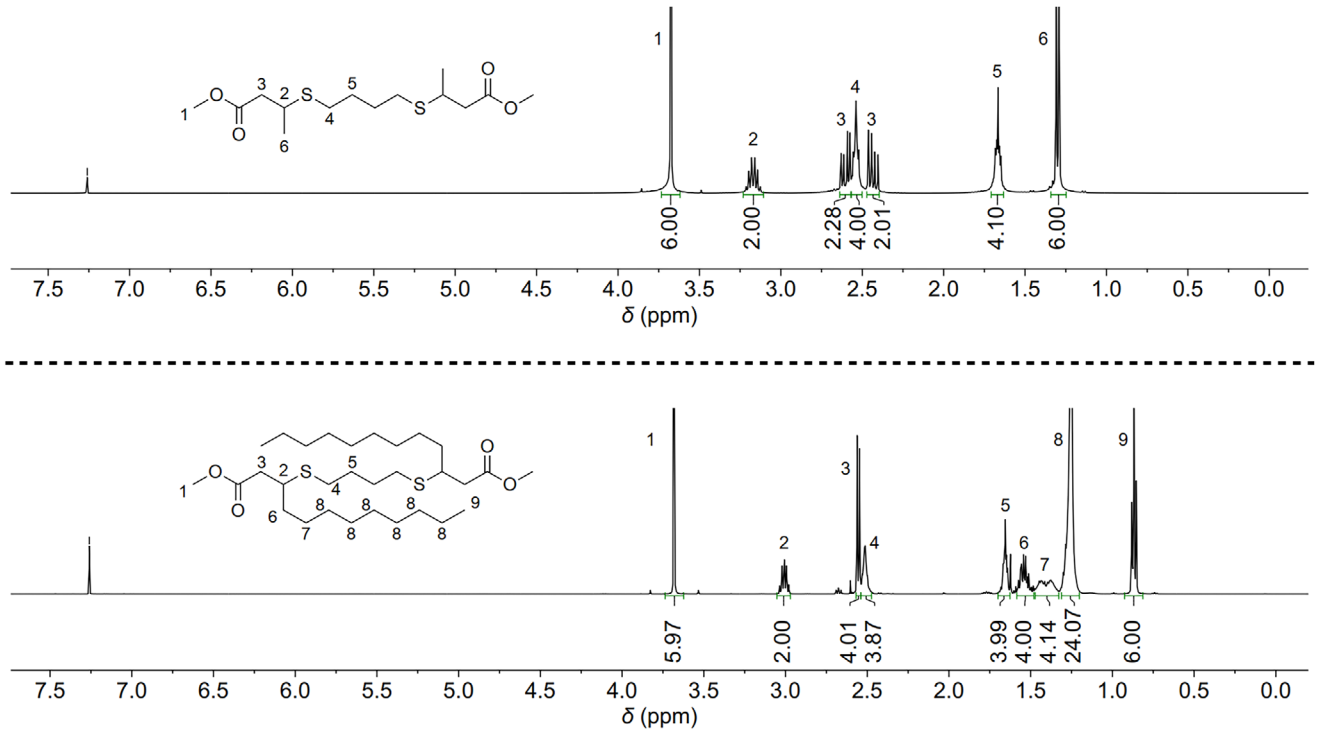

FIGURE 1 | Stacked ^{1}H NMR spectra of methyl crotonate dimer CD1 (top) and methyl laurate dimer LD1 (bottom) in $CDCl_3$. NMR, nuclear magnetic resonance.

In summary, the reaction sequence of dehydrogenation, esterification, and thia-Michael addition was performed successfully with 40 g of lauric acid. The product **LD1** was isolated in an overall yield of 27%, and it was demonstrated that 51% of the unreacted lauric acid could be recovered as methyl laurate by distillation. The development of this reaction sequence ultimately allowed the preparation of three fatty acid–based dimethyl esters (**LD1**–**LD3**) for the synthesis of renewable polyesters (Scheme 2). It should however be noted here that the samples of **LD1**–**LD3** that were actually used for polymerizations were synthesized via a different reaction pathway, as optimization of the dehydrogenation and the polymerizations themselves were conducted in parallel in the laboratory. Hence, α,β-unsaturated lauric acid was synthesized from decanal and malonic acid via a Knoevenagel–Doebner condensation [27]. Esterification with methanol and subsequent thia-Michael additions yielded **LD1–LD3** (Section 1.7). The analytic data of the final products derived from the two different synthesis routes are identical.

Renewable 1,12-dodecanediol was polymerized with methyl laurate–based dimers **LD1–LD3** to synthesize bio-based polyesters **LD-P1**–**LD-P3** (Scheme 2, bottom) [25]. In addition, **CD1**–**CD3** were polymerized with 1,12-dodecanediol as well to synthesize analogous polymers that differ from the methyl laurate polymers only in the length of the side chain in the repeating unit (C_1 vs. C_9) (**CD-P1**–**CD-P3**). The influence of the long C_9 side chain on the thermal properties of the polymers was afterward evaluated by comparing each **LD** polymer with its respective **CD** polymer analogue.

All polymerizations were performed solvent-free with 5 mol% of titanium(IV) isopropoxide and applying a temperature/pressure gradient starting at 140°C and 700 mbar and ending at 200°C and 10 mbar to remove the condensation product methanol and to achieve full conversion. In SEC, high average molecular weights (M_n) ranging from 26.0 to 31.8 kDa and dispersities ($Đ$) from 1.75 to 1.85 were obtained for polymers **LD-P1**–**LD-P3** (Table 4). Polymerizations of **CD1**–**CD3** resulted in lower M_n values between 13.0 and 29.1 kDa and dispersities of 1.52–1.74. The molecular weight of all polymers was furthermore estimated via ^{1}H NMR spectroscopy by integration of the end group signals of methyl esters and hydroxymethyl groups at 3.69 and 3.63 ppm, respectively (Table 4, see Section 1.7 for experimental data). The M_n values obtained by ^{1}H NMR spectroscopy deviated from the respective SEC results by 2%–25% and confirmed high molecular weight polycondensates. The results from ^{1}H NMR spectroscopy moreover revealed that every **LD** polymer had a higher M_n than its respective **CD** polymer (Section 1.7).

The temperature of 5 wt% loss ($T_{d,5\%}$) determined by TGA increased incrementally from **LD-P1** with the short 1,4-butanedithiol linker (332°C) to **LD-P3** with the longer 1,10-decanedithiol linker (345°C). The same trend was observed for the methyl crotonate–based polymers (from 306 to 336°C), indicating that a higher relative content of methylene groups improved thermal stability. Moreover, it was noted that every **LD** polymer had an improved $T_{d,5\%}$ value (up to 20°C higher) than the respective **CD** polymer (Table 4). This indicates that also the longer side chain had a positive influence on the thermal stability of the materials.

At last, DSC experiments were performed to evaluate the influence of the nonyl side chains on the thermal properties of the

TABLE 4 | Synthesized polyesters from methyl crotonate and methyl laurate-based dimethyl esters (CD1–CD3, LD1–LD3) and 1,12-dodecanediol together with their average molar mass (M_n), dispersity ($Đ$), temperature of 5 weight% loss ($T_{d,5\%}$), and melting temperature (T_m).

Polymer	M_n (SEC) (kDa)	$Đ$	M_n (NMR) (kDa)	$T_{d,5\%}$ (°C)	T_m (°C)
CD-P1	20.6	1.52	26.3	306	10
LD-P1	31.8	1.75	27.4	332	−31 and 16
CD-P2	13.0	1.71	12.2	321	13
LD-P2	28.1	1.85	35.7	341	—
CD-P3	29.1	1.74	21.8	334	36
LD-P3	26.0	1.83	25.6	344	0 and 15

Abbreviations: NMR, nuclear magnetic resonance; SEC, size exclusion chromatography.

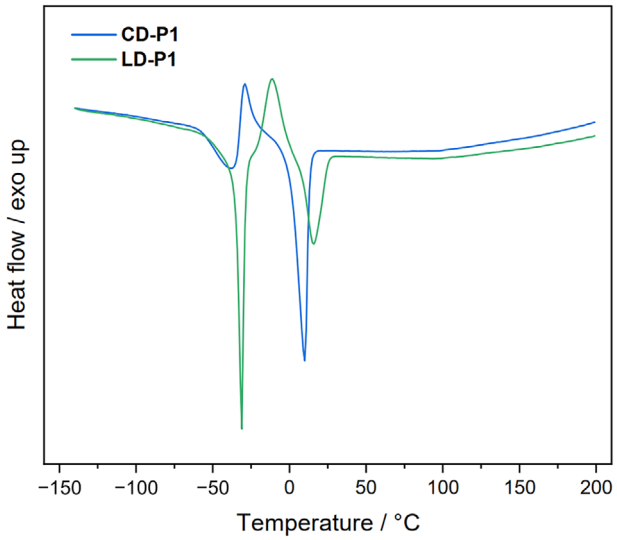

FIGURE 2 | DSC measurements of CD-P1 and LD-P1 (second heating run). DSC, differential scanning calorimetry.

polymers. Exemplarily, DSC measurements of **CD-P1** and **LD-P1** are depicted in Figure 2.

For Polymer **CD-P1**, a glass transition temperature (T_g) of −44°C and a cold crystallization at −29°C together with a melting point at 10°C were observed. Cold crystallization and melting point were observed as well for polymer **LD-P1** at slightly higher temperatures of −11 and 16°C, respectively. Moreover, one additional melting point was observed at −31°C, which most likely originates from the crystallization of the nonyl side chains. The crystallization of side chains was reported in several studies for polymers with long aliphatic side chains [8, 9, 37, 38]. For instance, Beiner et al. observed a melting point at −26°C for poly(*n*-lauryl methacrylate) with a C_{12} side chain, whereas no melting point was detected for (*n*-decyl methacrylate) with a C_{10} side chain. In another study by Meier et al., side chain crystallization was observed for a malonate-derived polyester with a side chain length of 10 carbon atoms at −36°C, which is similar to the herein observed melting point at −31°C. The side chain crystallization effect was, however, not observed for the other two fatty acid–based polymers. A low T_g of −50°C and no melting point at all were observed for **LD-P2,** whereas **CD-P2** had a T_g at −52°C and a melting point at 13°C (Figure S46). Interestingly, **CD-P3** exhibited a higher T_g and melting point of −30°C and 36°C, respectively (Figure S52). The long side chain analogue **LD-P3** exhibited a lower T_g of −40°C and two melting points at 0°C and 15°C, respectively. It is therefore possible to alter thermal transitions of these polymers by replacement of short side chains with longer ones.

4 | Conclusions

In the present work, a new three-step reaction sequence was developed for the synthesis of bio-based dimethyl esters and their polyesters starting from renewable saturated fatty acids. The sequence consists of a catalytic dehydrogenation with molecular oxygen as oxidant, an esterification with methanol, and a dimerization reaction with dithiols via thia-Michael addition. A recently established method for the catalytic dehydrogenation of carboxylic acids was thus utilized for the synthesis of α,β-unsaturated lauric acid [12]. The original procedure was first optimized considering sustainability aspects to exclude solvents, co-catalysts, and overstoichiometric amounts of inorganic bases, thereby reducing the amount of waste formed immensely. The dehydrogenation was performed on a 40 g scale to obtain a mixture consisting of 60% lauric acid and 40% α,β-unsaturated lauric acid, which was directly esterified in a second step with methanol and catalytic amounts of sulfuric acid to obtain a mixture of the respective methyl esters in quantitative yield. A subsequent thia-Michael addition with 1,4-butanedithiol allowed not only the synthesis of a new fatty acid–based dimethyl ester in a yield of 27% over all three reactions, but also the recovery of 51% of the initially used lauric acid in the dehydrogenation step as methyl laurate. The developed reaction sequence is thus quite sustainable, as waste generation is kept to a minimum. The sequence further allows the use of otherwise difficult-to-functionalize saturated fatty acids. The thia-Michael addition was moreover performed with 1,6-hexanedithiol and 1,10-decanedithiol to produce two more dimethyl esters with longer aliphatic linkers between both ester groups. At last, all dimethyl esters were polymerized with 1,12-dodecanediol to produce bio-based polyesters with high molecular weights ranging from 26.0 to 31.8 kDa. The influence of the long C_9 side chain on the thermal properties of the materials was evaluated by comparison of each polymer with its analogous methyl crotonate–based polymer bearing only a short methyl side chain. It was observed that the long side chain had a positive impact on the thermal stability of all polymers, as the temperature

of 5 wt% loss increased by up to 20°C compared to the polymers with methyl side chains. Generally, it was possible to alter the thermal properties of these materials by incorporating longer side chains into the polymer repeating unit.

Acknowledgments

The authors thank Prof. Dr. Stefan Bräse, Prof. Dr. Jörg Lahann, Prof. Dr. Patrick Théato, and Birgit Huber for TGA measurements; Prof. Dr. Patrick Théato and Dr. Azra Kocaarslan for DSC measurements; Lara Hirsch for mass spectrometric measurements; and Silas Leidenheimer for his help on the synthesis of the ligand.

Conflicts of Interest

The authors declare no conflicts of interest.

Data Availability Statement

The author has provided the required data availability statement and, if applicable, included functional and accurate links to said data therein.

References

1. "Plastics—the Fast Facts 2023", PlasticsEurope. published 2023, https://plasticseurope.org/knowledge-hub/plastics-the-fast-facts-2023/.

2. L. Montero de Espinosa and M. A. R. Meier, "Plant Oils: The Perfect Renewable Resource for Polymer Science?!," *European Polymer Journal* 47 (2011): 837–852.

3. S. Pandey, B. S. Rajput, and S. H. Chikkali, "Refining Plant Oils and Sugars to Platform Chemicals, Monomers, and Polymers," *Green Chemistry* 23 (2021): 4255–4295.

4. J. C. Ronda, G. Lligadas, M. Galià, and V. Cádiz, "Vegetable Oils as Platform Chemicals for Polymer Synthesis," *European Journal of Lipid Science and Technology* 113 (2011): 46–58.

5. W. S. Port, J. E. Hansen, E. F. Jordan Jr., T. J. Dietz, and D. Swern, "Polymerizable Derivatives of Long-Chain Fatty Acids. IV. Vinyl Esters," *Journal of Polymer Science* 7 (1951): 207–220.

6. H. M. Teeter, "Vinyl Monomers Derived From Fats and Oils," *Journal of the American Oil Chemists Society* 40 (1963): 143–156.

7. D. Heinze, T. Mang, C. Popescu, and O. Weichold, "Effect of Side Chain Length and Degree of Polymerization on the Decomposition and Crystallization Behaviour of Chlorinated Poly(Vinyl Ester) Oligomers," *Thermochimica Acta* 637 (2016): 143–153.

8. H. Mutlu and M. A. R. Meier, "Ring-Opening Metathesis Polymerization of Fatty Acid Derived Monomers," *Journal of Polymer Science, Part A: Polymer Chemistry* 48 (2010): 5899–5906.

9. N. Kolb and M. A. R. Meier, "Monomers and Their Polymers Derived From Saturated Fatty Acid Methyl Esters and Dimethyl Carbonate," *Green Chemistry* 14 (2012): 2429–2435.

10. R. Quermann, R. Maletz, and H. J. Schäfer, "Conversion of Fatty Acids and Derivatives, IV. Conversion of Fatty Acid Methyl Esters Into Dialkylated Succinic Esters by Oxidative Coupling of Their Enolates," *Liebigs Annalen Der Chemie* 1993 (1993): 1219–1223.

11. Y. Zhao, Y. Chen, and T. R. Newhouse, "Allyl-Palladium-Catalyzed α,β-Dehydrogenation of Carboxylic Acids via Enediolates," *Angewandte Chemie International Edition* 56 (2017): 13122–13125.

12. Z. Wang, L. Hu, N. Chekshin, et al., "Ligand-Controlled Divergent Dehydrogenative Reactions of Carboxylic Acids via C–H Activation," *Science* 374 (2021): 1281–1285.

13. B. D. Mather, K. Viswanathan, K. M. Miller, and T. E. Long, "Michael Addition Reactions in Macromolecular Design for Emerging Technologies," *Progress in Polymer Science* 31 (2006): 487–531.

14. D. P. Nair, M. Podgórski, S. Chatani, et al., "The Thiol-Michael Addition Click Reaction: A Powerful and Widely Used Tool in Materials Chemistry," *Chemistry of Materials* 26 (2014): 724–744.

15. P. Wadhwa, A. Kharbanda, and A. Sharma, "Thia-Michael Addition: An Emerging Strategy in Organic Synthesis," *Asian Journal of Organic Chemistry* 7 (2018): 634–661.

16. M. Bandini, P. G. Cozzi, M. Giacomini, P. Melchiorre, S. Selva, and A. Umani-Ronchi, "Sequential One-Pot InBr3-Catalyzed 1,4-Then 1,2-Nucleophilic Addition to Enones," *Journal of Organic Chemistry* 67 (2002): 3700–3704.

17. S. K. Garg, R. Kumar, and A. K. Chakraborti, "Copper(II) Tetrafluoroborate as a Novel and Highly Efficient Catalyst for Michael Addition of Mercaptans to α,β-Unsaturated Carbonyl Compounds," *Tetrahedron Letters* 46 (2005): 1721–1724.

18. H. Firouzabadi, N. Iranpoor, and A. A. Jafari, "$H3PW_{12}O_{40}$ as a Useful Recyclable Heterogeneous Catalyst for the Facile and Highly Efficient Michael Addition Reaction of Thiols to α,β-Unsaturated Ketones," *Synlett* 2 (2005): 299–303.

19. D. M. Pore, M. S. Soudagar, U. V. Desai, T. S. Thopate, and P. P. Wadagaonkar, "Potassium Phosphate or Silica Sulfuric Acid Catalyzed Conjugate Addition of Thiols to α,β-Unsaturated Ketones at Room Temperature Under Solvent-Free Conditions," *Tetrahedron Letters* 47 (2006): 9325–9328.

20. J. W. Chan, C. E. Hoyle, A. B. Lowe, and M. Bowman, "Nucleophile-Initiated Thiol-Michael Reactions: Effect of Organocatalyst, Thiol, and Ene," *Macromolecules* 43 (2010): 6381–6388.

21. D. Zhang, M.-J. Dumont, and A. Cherestes, "An Efficient Strategy for the Synthesis of 5-Hydroxymethylfurfural Derivative Based Poly(β-Thioether Ester) via Thiol-Michael Addition Polymerization," *RSC Advances* 6 (2016): 83466–83470.

22. N. Azizi, A. Khajeh-Amiri, H. Ghafuri, and M. Bolourtchian, "A Highly Efficient, Operationally Simple and Selective Thia-Michael Addition Under Solvent-Free Condition," *Green Chemistry Letters and Reviews* 2 (2009): 43–46.

23. M. Winkler, Y. S. Raupp, L. A. M. Köhl, H. E. Wagner, and M. A. R. Meier, "Modified Poly(ε-Caprolactone)s: An Efficient and Renewable Access via Thia-Michael Addition and Baeyer–Villiger Oxidation," *Macromolecules* 47 (2014): 2842–2846.

24. O. Daglar, B. Ozcan, U. S. Gunay, G. Hizal, U. Tunca, and H. Durmaz, "Extremely Rapid Postfunctionalization of Maleate and Fumarate Main Chain Polyesters in the Presence of TBD," *Polymer* 182 (2019): 121844.

25. M. M. Ahsan, S. Sung, H. Jeon, M. D. Patil, T. Chung, and H. Yun, "Biosynthesis of Medium- to Long-Chain α,ω-Diols From Free Fatty Acids Using CYP153A Monooxygenase, Carboxylic Acid Reductase, and *E. coli* Endogenous Aldehyde Reductases," *Catalysts* 8 (2018): 4.

26. W. C. Still, M. Kahn, and A. Mitra, "Rapid Chromatographic Technique for Preparative Separations With Moderate Resolution," *Journal of Organic Chemistry* 43 (1978): 2923–2925.

27. I. Galleano, M. Schiedel, M. Jung, A. S. Madsen, C. A. Olsen, and A. Continuous, "Fluorogenic Sirtuin 2 Deacylase Assay: Substrate Screening and Inhibitor Evaluation," *Journal of Medicinal Chemistry* 59 (2016): 1021–1031.

28. Sigma-Aldrich Chemie GmbH. *N,N-Dimethylformamide; MSDS Product Number 227056* (Merck KGaA, 2024), https://www.sigmaaldrich.com/DE/en/product/sial/227056.

29. Sigma-Aldrich Chemie GmbH. *p-Benzoquinone; MSDS Product Number B10358* (Merck KGaA, 2024), https://www.sigmaaldrich.com/DE/en/product/sial/b10358.

30. R. K. Henderson, C. Jiménez-González, D. J. C. Constable, et al., "Expanding GSK's Solvent Selection Guide—Embedding Sustainability

Into Solvent Selection Starting at Medicinal Chemistry," *Green Chemistry* 13 (2011): 854–862.

31. C. M. Alder, J. D. Hayler, R. K. Henderson, et al., "Updating and Further Expanding GSK's Solvent Sustainability Guide," *Green Chemistry* 18 (2016): 3879–3890.

32. W.-X. Wu, "Lipase-Catalyzed Synthesis of Aliphatic Poly(*β*-Thioether Ester) With Various Methylene Group Contents: Thermal Properties, Crystallization and Degradation," *Polymer International* 68 (2019): 1848–1855.

33. R. Sanaa, D. Portinha, R. Medimagh, and E. Fleury, "Synthesis of Linear and Crosslinked Isosorbide-Containing Poly(*β*-Thioether Ester) via Amine-Catalyzed Thiol-Michael Addition," *European Polymer Journal* 220 (2024): 113498.

34. Sigma-Aldrich Chemie GmbH. *1,8-Diazabicyclo[5.4.0]Undec-7-Ene; MSDS Product Number 8.03282* (Merck KGaA, 2024), https://www.sigmaaldrich.com/DE/en/product/mm/803282.

35. Sigma-Aldrich Chemie GmbH. *1,1,3,3-Tetramethylguanidine; MSDS Product Number 241768* (Merck KGaA, 2023), https://www.sigmaaldrich.com/DE/en/product/aldrich/241768.

36. R. K. Henderson, A. P. Hill, A. M. Redman, and H. F. Sneddon, "Development of GSK's Acid and Base Selection Guides," *Green Chemistry* 17 (2015): 945–949.

37. E. Hempel, H. Huth, and M. Beiner, "Interrelation Between Side Chain Crystallization and Dynamic Glass Transitions in Higher Poly(n-Alkyl Methacrylates)," *Thermochimica Acta* 403 (2003): 105–114.

38. G. Çayli and M. A. R. Meier, "Polymers From Renewable Resources: Bulk ATRP of Fatty Alcohol-Derived Methacrylates," *European Journal of Lipid Science and Technology* 110 (2008): 853–859.

Supporting Information

Additional supporting information can be found online in the Supporting Information section.